Ultra-distal Kamchatkan ash on Arctic Svalbard: towards hemispheric cryptotephra correlation

Willem G.M. van der Bilt [ab1], *Christine S. Lane* [c] *& Jostein Bakke* [ab]

[a] Department of Earth Science, University of Bergen, Allégaten 41, 5007, Bergen, Norway

[b] Bjerknes Centre for Climate Research, Bergen, Norway

[c] Department of Geography, University of Cambridge, Downing Place, CB2 3EN, Cambridge, United Kingdom

Keywords: Holocene, cryptotephra, Arctic, Pacific, Svalbard

[1] Corresponding author, Department of Earth Science, University of Bergen, Allégaten 41, 5007, Bergen, Norway. E-mail address: willemvanderbilt@gmail.comwillemvanderbilt@gmail.com

Abstract

Rapidly deposited and geochemically distinct volcanic ash (tephra) markers represent a powerful chronological tool that enables precise dating and correlation of geological archives. Recent analytical advances now allow fingerprinting of non-visible ash (cryptotephra) over thousands of kilometers. This has opened up tantalizing possibilities for the intercontinental synchronization of records. We present geochemical evidence to demonstrate that ash from a Svalbard lake sediment core correlates to the Kamchatkan KS_2 eruption. By expanding the known dispersal range of cryptotephra by thousands of kilometers and linking the Pacific and Atlantic Arctic, this study raises cryptotephra analysis to a new level. Also, the presented findings mark a step towards a hemispheric tephrochronological framework. Finally, this study highlights the importance of looking beyond proximal volcanic sources to find a correlation.

1 Introduction

Volcanic ashes (tephra) represent time-parallel markers (isochrons) that provide a unique means of precisely dating and correlating geological archives (Lowe, 2011). This powerful geochronological tool enables synchronization of paleoclimate records over millennia across distances of thousands of kilometers (Blockley et al., 2014). Apart from anchoring events in time, tephrochronology is invaluable to constrain phase relationship between components of the climate system (e.g. Lane et al., 2013a).

In recent years, key analytical advances have enabled robust geochemical fingerprinting of non-visible glass shards (cryptotephra) (Blockley et al., 2005; Hayward, 2011; Turney, 1998b). As a result, ash markers are detected at increasingly large distances from their respective volcanic source, expanding existing tephrochronological frameworks (Davies, 2015). Indeed, several recent studies correlate tephra markers between continents (Bourne et al., 2016; De Silva and Zielinski, 1998; Jensen et al., 2014; Lane et al., 2012; Lane et al., 2013b; Mackay et al., 2016; McLean et al., 2016; Pearce et al., 2014; Song et al., 2000; Sun et al., 2014; Tomlinson et al., 2012 and references therein; Zdanowicz et al., 1999).

Yet, despite recent advances, the potential of this technique remains underutilized across large geographical areas (Machida, 2002). These include the High Arctic, where tephrochronology could contribute significantly as a scarcity of organic material often precludes radiocarbon dating. Tephra-based synchronization of regional paleoclimate records may help understand the causes of the amplified response of Arctic climate to change (Serreze and Barry, 2011).

We report detection of a Kamchatkan-sourced discrete ash layer in a lake sediment sequence from the High Arctic Svalbard archipelago (79°N). Geochemical analysis of shards using an electron microprobe enabled us to correlate this horizon to the KS_2 eruption ~7000 cal. yr BP. This ultra-distal find raises cryptotephra analysis to a new level by linking the Pacific and Atlantic Arctic over up to ~14,000 km.

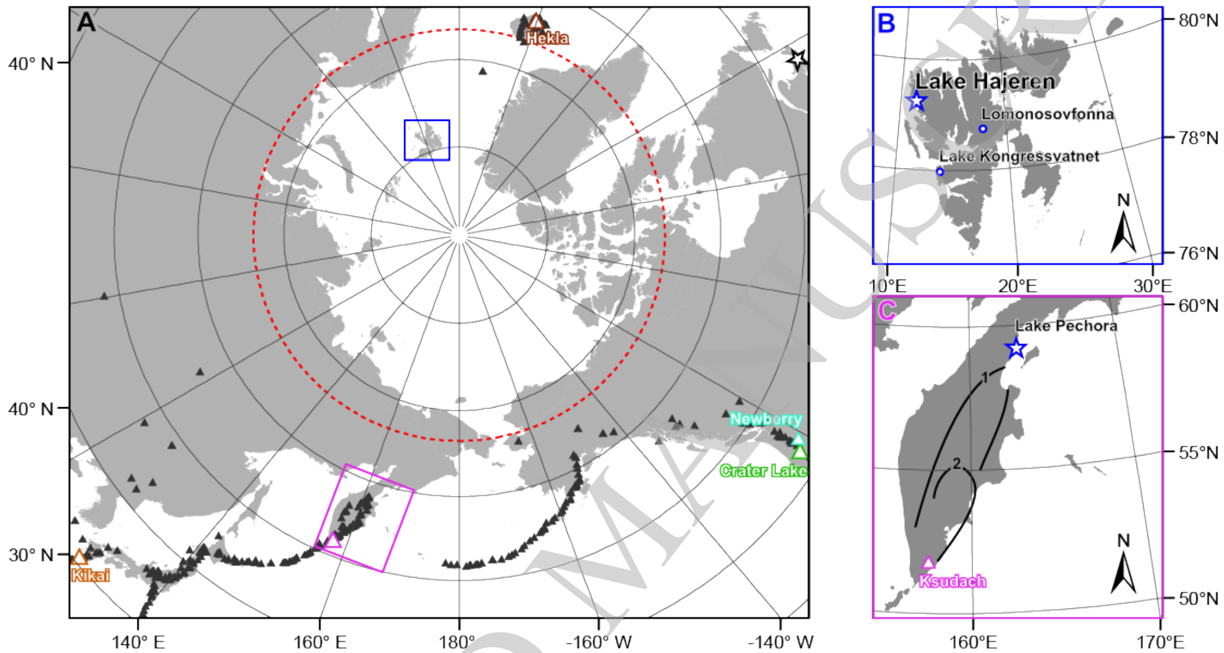

Fig. 1. A: Pan-arctic overview, showing volcanoes that have been active during the Holocene in black triangles after USGS (2005) as well as those discussed in this paper as color-coded triangles: Crater Lake (blue), Hekla (brown), Kikai (orange), Ksudach (pink) and Newberry (green). The dashed red line marks the Arctic Circle while the pink and blue rectangles outline insets B and C, respectively. The open star highlights the only other extra-regional site where KS_2 ash has been found (S. Pyne-O'Donnell, pers. comm.). **B:** the Svalbard archipelago, indicating the location of Lake Hajeren with a star. Blue circles highlight the localities of previous tephra finds on Spitsbergen, Lake Kongressvatnet (D'Andrea et al., 2012) and Lomonosovfonna Ice Cap (Kekonen et al., 2005). **C:** close-up of the Kamchatka peninsula, highlighting the Ksudach volcano in pink and delineating 1 and 2 cm isopachs of the KS_2 tephra after Kyle et al. (2011). The blue star indicates the location of mentioned Lake Pechora.

2 Setting

Our study site, Lake Hajeren, is a small (0.23 km^2) basin located on the Svalbard archipelago (79.26°N, 11.52°E, 35 m a.s.l) in the Arctic-Atlantic (Figs. 1a-b). The surrounding catchment covers 2.96 km^2, hosts two cirque glaciers and mostly comprises gently sloping terrain that minimizes exposure to mass-wasting processes (van der Bilt et al., 2016b). With a recorded average temperature of -5 °C (Nordli, 2010), the lake is typically frozen for ~10 months a year. The sediment core sampled for this study (HAP0212) has been extracted from the basin`s deep (~19 m) and flat center. This Holocene-length laminated sequence has been previously studied: details pertaining to core extraction and radiocarbon dating are described in van der Bilt et al. (2015a) and van der Bilt et al. (2016a). Previous cryptotephra studies on Svalbard report Late Holocene (past 2 kyrs) horizons from the second closest volcanic source region Iceland (D’Andrea et al., 2012; Kekonen et al., 2005), ~1800 km to the South (Fig. 1a).

3 Methods

Cryptotephra glass was separated from sediments using the flotation procedure of Turney (1998a) and Blockley et al. (2005) by sieving (> 15 μm) and density extraction (1.95-2.55 g/cm^3). We scanned the entire core length (332.5 cm) for shards by applying a three-phase routine. First, contiguous 10 cm vertical intervals were analyzed to identify core sections with glass shards. For this purpose, samples were mounted in Canada balsam and examined under a light microscope (×200). Next, we zoomed in on intervals with tephra shards at a 1 cm resolution using the same approach. Finally, we re-investigated the horizon discussed in this paper, to pick individual shards for geochemical analysis. To this end, we used a gas chromatography syringe (cf. Lane et al., 2014).

To fingerprint shards geochemically, we measured major and minor element oxide concentrations using wavelength dispersive X-Ray spectrometer electron microprobe (WDS-EMP) analysis. Analyses were carried out at **1**) the Research Laboratory for Archaeology and the History of Art at the University of Oxford with a JEOL JXA-8600, using an accelerating voltage of 15 kV, a 6 nA beam current and a 10 µm beam size, and **2**) the Electron Probe Microanalysis Facility at the School of Geosciences of the University of Edinburgh with a Cameca SX100, using an accelerating voltage of 15 kV, beam currents of 0.5 nA (Na/Al), 2 nA (Mg/Si/K/Fe/Ca) and 60 nA (P/Ti/Mn) and a 6 µm beam size. As Chlorine (Cl) was not measured in Edinburgh, we removed it from our dataset prior to normalization for comparison purposes. Both instruments were calibrated using a suite of characterized mineral standards, while secondary glass standards were analyzed between and within runs to monitor analytical precision. Unnormalized glass compositional data, including means and standard deviations, for sample and secondary standard measurements are provided in Tables S1-2.

To help identify the source eruption of the presented horizon, we complemented bivariate plots with Principal Component Analysis (PCA), an ordination technique often used to identify (dis)similarities between sample groups (Birks et al., 2012). PCA combines data on the variability of all measured oxides, providing more information to help distinguish between volcanic sources than bivariate plots. To permit PCA on closed compositional tephra oxide concentrations, we log-transformed data after Aitchison (1986). Following the recommendations of Pollard et al. (2006), we employed the centered log-ratio approach, dividing the natural log of element oxide values by that of the geometric sample mean after data normalization c.f. Pearce et al. (2008). PCA analysis was then carried out using the CANOCO 5 software (Ter Braak, 1988), scaling and centering sample scores in the ensuing ordination diagram to highlight correlations (Šmilauer and Lepš, 2014). Finally, to further assess (dis)similarity between volcanic sources, we calculated prediction ellipses around PCA sample scores and bivariate oxide concentrations at a 95% confidence interval c.f. Pouget et al. (2014). For this purpose, we used the CAR package in version 3.0.1 of the R environment (Fox et al., 2016; RCoreTeam, 2014).

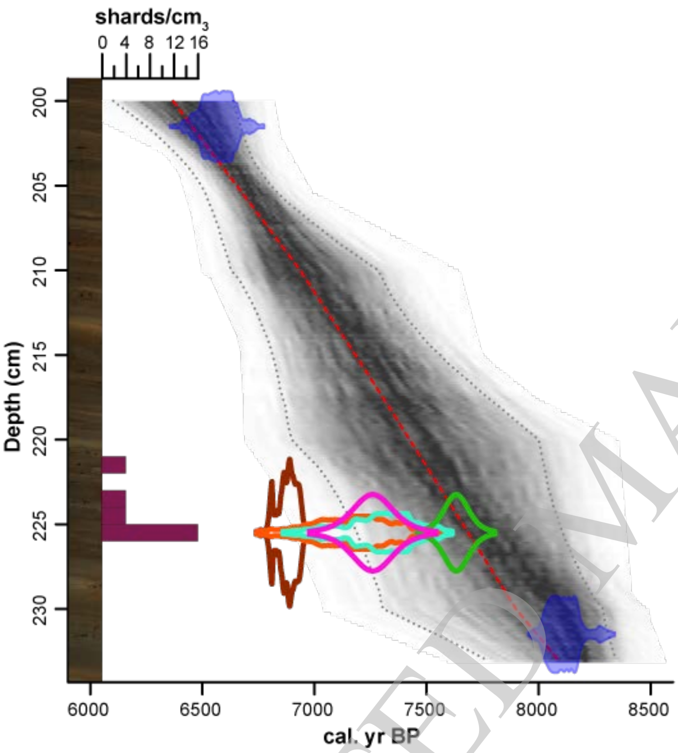

Fig. 2. A photographic image and counted tephra shards for the discussed interval of core HAP0212, plotted together with the radiocarbon-based age-depth model by van der Bilt et al. (2015b), which is bracketed by two ages (filled-blue probability density functions). In addition to the weighted mean (red dashed line), 95% confidence limits of the model are marked (stippled gray line). The shaded area indicates the density of age-depth iterations. Also shown are the published probability density functions for the calibrated ages of eruptions discussed in the text (Table 1): the Mazama eruption that formed Crater Lake (light blue), Lairg A from Hekla (brown), the Akahoya eruption of the Kikai caldera (K-Ah) (orange), KS_2 from Ksudach volcano (pink) and the East Lake tephra, formed during the Interlake Eruptive Episode of Newberry volcano (green).

4 Results and discussion

We analyzed six glass shards in a maximum concentration of 16 shards per cm^3 of sediment between 225 and 226 cm core depth. As can be seen in Fig. 2, this maximum marks a sharp concentration peak, allaying concerns of reworking (Pyne-O'Donnell, 2011). We therefore place the isochron at 225.5 cm. Glass shards are vesicular and colorless and measure ~20-40 μm. Analyzed shards reveal a dacitic composition, with SiO_2 concentrations ranging between 66.97-70.18%, and low K_2O concentrations (1.18-1.29%) (Table S1) (Figs. 3a & S1). The radiocarbon chronology for Lake Hajeren by van der Bilt et al. (2016a) brackets deposition between 8104 – 7152 cal. BP (95% confidence limits) (Fig. 2). If geochemically fingerprinted, the discussed isochron could reduce this uncertainty range. Owing to a number of recent intercontinental cryptotephra correlations (e.g. Bourne et al., 2016; Mackay et al., 2016; McLean et al., 2016), we also consider distant volcanic sources to correlate the presented tephra. Considering coincident proximal as well as large explosive (Volcanic Explosivity Index: VEI > 5) distal eruptions (volcanoes) with an ash dispersal axis towards Svalbard, we identify five potential candidates (Figs. 1a & 2) (Table 1): the Mazama (Crater Lake), East Lake (Newberry), Kikai-Akahoya (Kikai) (K-Ah), KS_2 (Ksudach) and Lairg A (Hekla) tephras (Kyle et al., 2011; Pilcher et al., 2005; Plunkett et al., 2015; Pyne-O'Donnell et al., 2012; Smith et al., 2013).

Plotting log-centered oxide geochemistry of reference material from these markers with that of our shards in an ordination diagram shows that composition of the presented marker is consistent with the KS_2 tephra (Fig. 4). Indeed, scores of our samples on the first two PCs, which explain 87% of dataset variance, plot within the 95% prediction ellipse of KS_2 reference material (Fig. 4). This correlation is supported by the bivariate plots of Fig. 3a-c, highlighting the diagnostic low K_2O content of Ksudach ash (Braitseva et al., 1997), and the typical high Al_2O_3 content of KS_2 tephra (Kyle et al., 2011). Again, the geochemistry of Lake Hajeren shards falls within the 95% prediction ellipse of KS_2 reference material.

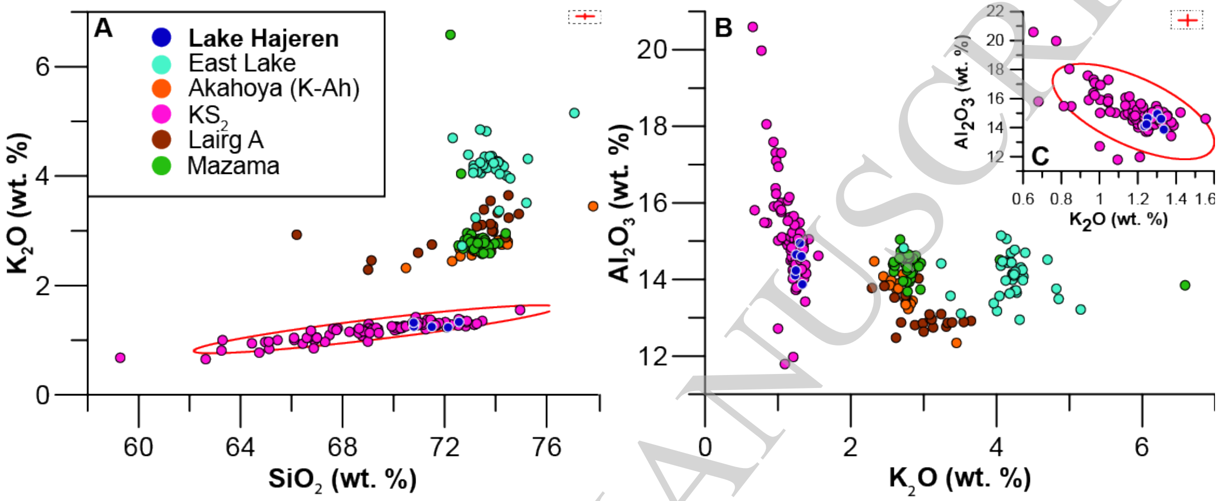

Fig. 3. Bivariate plots that compare the normalized geochemical composition of discussed eruptions to analyzed shards from Lake Hajeren – **A:** SiO_2 vs. K_2O, **B:** K_2O vs. Al_2O_3 and C: K_2O vs. Al_2O_3 for KS_2 reference material In-set red crosses mark the analytical uncertainty of measurements, based on the pooled and weighted 2σ of secondary standard analyses (also see Tables S1-2). 95% prediction ellipses are drawn around KS_2 reference material.

Tephra	Volcano	Dispersal	Published age	Reference
Akahoya (K-Ah)	Kikai	NE	7434 – 6885 cal. yr BP	Machida and Arai (2003)*
East Lake	Newberry	E	7519 – 7144 cal. yr BP	MacLeod et al. (1995)*
KS_2	Ksudach	N	7340 – 7180 cal. yr BP	Plunkett et al. (2015)
Lairg A	Hekla	N	6946 – 6841 cal. yr BP	Pilcher et al. (1996)*
Mazama	Crater Lake	NE	7682 – 7584 cal. yr BP	Egan et al. (2015)

Table 1. The volcanic source, reported dispersal axes and published age ranges of discussed eruptions. * highlight reported ^{14}C ages that have been calibrated (95% range) with Clam 2.2 (Blaauw, 2010), using the IntCal13 calibration curve (Reimer et al., 2013).

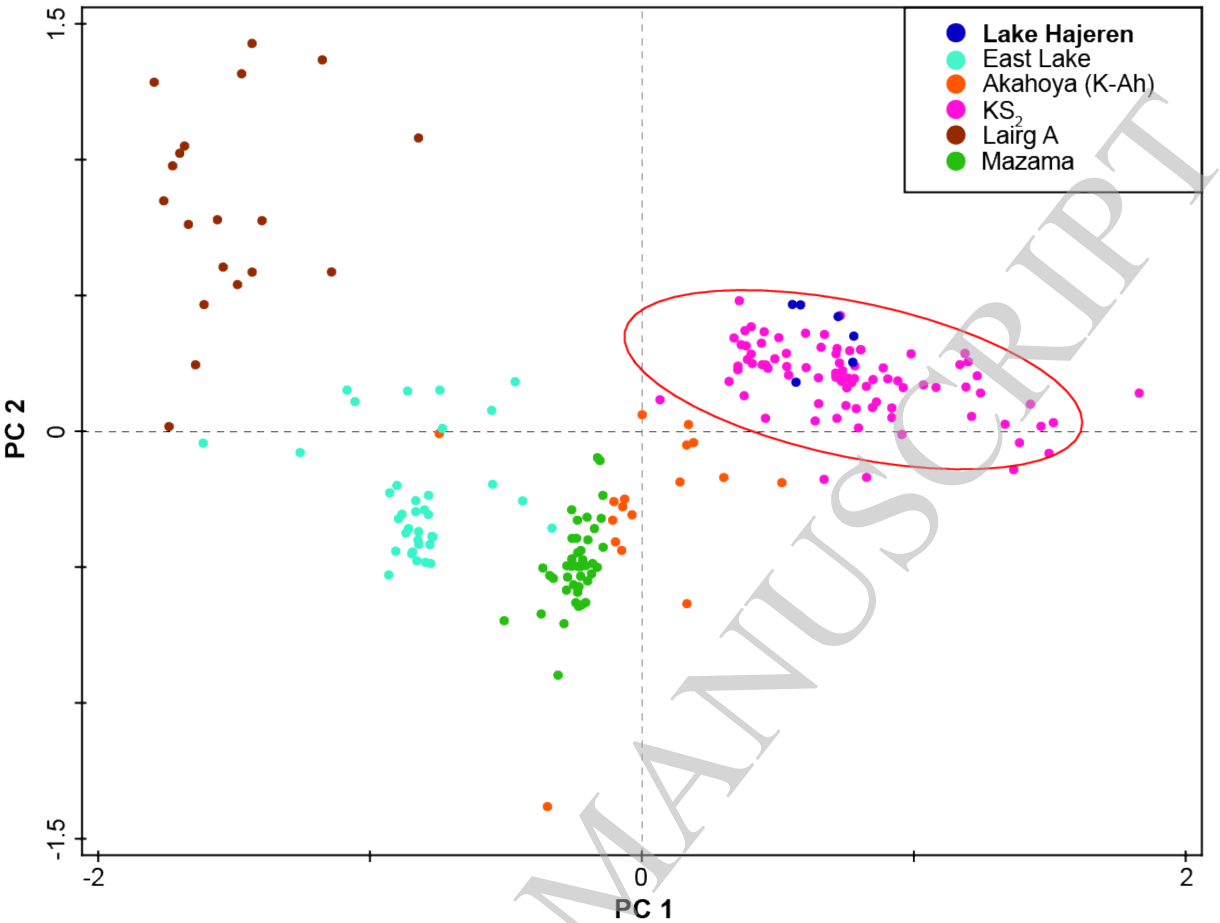

Fig. 4. Ordination diagram, showing log-centered scaled sample scores of geochemical oxide data from our samples and reference tephra compositions from discussed eruptions (see legend for color-coding) on the first two ordination axes or Principal Components (PCs). 95% prediction ellipses are drawn around plotted KS_2 reference material to highlight similarities.

Ksudach (51.8°N, 157.53°E) is a 1079 m a.s.l. high shield-like polygenetic edifice crowned with five nested calderas (Volynets et al., 1999), located on Russia's Kamchatka peninsula (Figs. 1a-c) and formed by major Late Pleistocene-Holocene eruptions (Melekestsev et al., 1996). KS_2 was one of the largest of these events, producing an estimated 7-8 km^3 of ejecta (Kyle et al., 2011; Volynets et al., 1999), dispersing visible ash up to 900 km northward and forming a prominent regional tephra marker (Plunkett et al., 2015) (Fig. 1c). Though closely spaced in time, the 7420 – 7255 cal. yr BP KS_3 eruption dispersed a much smaller ash volume of different (rhyodacitic) composition to the west of Ksudach (Braitseva et al., 1997; Kyle et al., 2011; Zaretskaya et al., 2007). Braitseva et al. (1997) first proposed an age for the KS_2 eruption of 6950-6740 cal. BP based on radiocarbon-dated soils and peat, but more recent dating efforts suggest an older age. We use the updated estimate of 7340-7180 cal. BP reported by Plunkett et al. (2015), which is based on bulk sediment ^{14}C ages from Lake Pechora, ~900 km north of Ksudach (Fig. 2c). This estimate is supported by Pendea et al. (2017), who model an age of 7204 cal. BP, based on radiocarbon-dated terrestrial macrofossils found directly below the KS_2 tephra. As shown in Fig. 2, the mean of this range falls within the 95% confidence limits of the radiocarbon-based age-depth model for Lake Hajeren by van der Bilt et al. (2016a) for the analyzed depth interval.

In summary, based on an indistinguishable major oxide geochemistry and coincident age, we claim that the presented cryptotephra horizon is sourced from the KS_2 eruption. Our discovery of Kamchatkan ash on Svalbard marks the first known example of a tephra that is found on three continents (Fig. 1a). Also, depending on the plume trajectory, this find increases the known dispersal range of cryptotephra by up to ~5000 of km (Fig. 1a).

Owing to the eastward path of the tropospheric westerlies- and stratospheric polar jet winds that prevail over Kamchatka, we argue that KS_2 ash was transported to Svalbard across North America and around the Arctic. This notion is supported by the only other known discovery of ultra-distal KS_2 cryptotephra, made in Nova Scotia (S. Pyne-O'Donnell, pers. comm.) (Fig. 1a). However, more finds are needed to constrain the plume trajectory of KS_2. A number of other factors may be invoked to help explain the exceptionally distal distribution of KS_2 ash towards Svalbard. The high water content of Ksudach magma, for example, which gives rise to a highly explosive eruption style that injects great volumes of ejecta high into the atmosphere (Volynets et al., 1999), allowing cryptotephra to remain aloft and be transported over vast distances following large events like KS_2. Additionally, distal dispersal from Kamchatka and deposition on Svalbard must have depended on favorable contemporaneous weather conditions. Notwithstanding the strength and position of dispersing atmospheric patterns, direct ash deposition in a High Arctic site like Hajeren is most likely during summer, when the lake catchment is ice and snow free (Davies et al., 2007; Pyne-O'Donnell, 2011). In this regard, it is worth noting that reconstructed summer temperatures in Lake Hajeren reached an optimum around the time of the KS_2 eruption (van der Bilt et al., 2016a), a period that marks the Atlantic-Arctic culmination of the Holocene Thermal Maximum (HTM) (Sejrup et al., 2016).

Indeed, coincidence with the HTM, a global time-transgressive climate event characterized by warmer-than-present conditions (Renssen et al., 2012), renders the KS_2 tephra highly relevant from a paleoclimate perspective. Our ultra-distal discovery of KS_2 ash opens possibilities to use this isochron to synchronize pan-Arctic paleoclimate records during the HTM, upscaling site-specific findings. Such an exercise will allow us to constrain lead-lag relationships in the Arctic climate system during a period that serves as a potential reference for the future. This may greatly enhance our understanding of the spatio-temporal signature of the region's amplified response to on-going warming (Miller et al., 2010).

In conclusion, the presented discovery of Kamchatka-sourced KS_2 ash on Arctic Svalbard raises cryptotephra analysis to a new level by **1**) expanding the known dispersal distance of cryptotephra, **2**) opening possibilities for pan-Arctic synchronization of paleoclimate records and **3**) providing a key building block for a hemispheric tephrochronological framework. Finally, this study emphasizes the need to consider ultra-distal sources to correlate deposits.

Acknowledgements

This study has received funding from the Norwegian Research Council through the project «Shifting Climate States of the Polar Regions» (210004) as well as the «INTIMATE» COST action (ES0907) and the *alminnelige naturvitenskapelige* Research Fund of the University of Bergen (UiB). We thank Rob D`Anjou, Bjørn Kvisvik and Torgeir Røthe for helping to retrieve the studied sediment cores. Finally, we like to express our gratitude to Victoria Cullen and Victoria Smith at RLAHA, University of Oxford, as well as Chris Hayward at the University of Edinburgh for their help with the geochemical analyses. Finally, we would like to express our gratitude to Vera Ponomareva and one anonymous reviewer for improving this manuscript with their comments.

References

Aitchison, J., 1986. The statistical analysis of compositional data.
Birks, H.J.B., Lotter, A.F., Juggins, S., Smol, J.P., 2012. Tracking environmental change using lake sediments: data handling and numerical techniques. Springer Science & Business Media.
Blaauw, M., 2010. Methods and code for 'classical' age-modelling of radiocarbon sequences. Quaternary Geochronology 5, 512-518.
Blockley, S.P.E., Bourne, A.J., Brauer, A., Davies, S.M., Hardiman, M., Harding, P.R., Lane, C.S., MacLeod, A., Matthews, I.P., Pyne-O'Donnell, S.D.F., Rasmussen, S.O., Wulf, S., Zanchetta, G., 2014. Tephrochronology and the extended intimate (integration of ice-core, marine and terrestrial records) event stratigraphy 8–128 ka b2k. Quaternary Science Reviews 106, 88-100.
Blockley, S.P.E., Pyne-O'Donnell, S.D.F., Lowe, J.J., Matthews, I.P., Stone, A., Pollard, A.M., Turney, C.S.M., Molyneux, E.G., 2005. A new and less destructive laboratory procedure for the physical separation of distal glass tephra shards from sediments. Quaternary Science Reviews 24, 1952-1960.
Bourne, A., Abbott, P., Albert, P., Cook, E., Pearce, N.J., Ponomareva, V., Svensson, A., Davies, S., 2016. Underestimated risks of recurrent long-range ash dispersal from northern Pacific Arc volcanoes. Scientific Reports 6.
Braitseva, O.A., Ponomareva, V.V., Sulerzhitsky, L.D., Melekestsev, I.V., Bailey, J., 1997. Holocene Key-Marker Tephra Layers in Kamchatka, Russia. Quaternary Research 47, 125-139.
D'Andrea, W.J., Vaillencourt, D.A., Balascio, N.L., Werner, A., Roof, S.R., Retelle, M., Bradley, R.S., 2012. Mild Little Ice Age and unprecedented recent warmth in an 1800 year lake sediment record from Svalbard. Geology 40, 1007-1010.
Davies, S.M., 2015. Cryptotephras: the revolution in correlation and precision dating. Journal of Quaternary Science 30, 114-130.

Davies, S.M., Elmquist, M., Bergman, J., Wohlfarth, B., Hammarlund, D., 2007. Cryptotephra sedimentation processes within two lacustrine sequences from west central Sweden. The Holocene 17, 319-330.

De Silva, S.L., Zielinski, G.A., 1998. Global influence of the AD 1600 eruption of Huaynaputina, Peru. Nature 393, 455-458.

Egan, J., Staff, R., Blackford, J., 2015. A revised age estimate of the Holocene Plinian eruption of Mount Mazama, Oregon using Bayesian statistical modelling. The Holocene, 0959683615576230.

Fox, J., Weisberg, S., Adler, D., Bates, D., Baud-Bovy, G., Ellison, S., Firth, D., Friendly, M., Gorjanc, G., Graves, S., 2016. Package 'car'.

Hayward, C., 2011. High spatial resolution electron probe microanalysis of tephras and melt inclusions without beam-induced chemical modification. The Holocene, 0959683611409777.

Jensen, B.J., Pyne-O'Donnell, S., Plunkett, G., Froese, D.G., Hughes, P.D., Sigl, M., McConnell, J.R., Amesbury, M.J., Blackwell, P.G., van den Bogaard, C., 2014. Transatlantic distribution of the Alaskan White River Ash. Geology 42, 875-878.

Kekonen, T., Moore, J., Perämäki, P., Mulvaney, R., Isaksson, E., Pohjola, V., van de Wal, R.S.W., 2005. The 800 year long ion record from the Lomonosovfonna (Svalbard) ice core. Journal of Geophysical Research: Atmospheres 110, D07304.

Kyle, P.R., Ponomareva, V.V., Rourke Schluep, R., 2011. Geochemical characterization of marker tephra layers from major Holocene eruptions, Kamchatka Peninsula, Russia. International Geology Review 53, 1059-1097.

Lane, C.S., Blockley, S.P., Mangerud, J., Smith, V.C., Lohne, Ø.S., Tomlinson, E., Matthews, I.P., Lotter, A., 2012. Was the 12.1 ka Icelandic Vedde Ash one of a kind? Quaternary Science Reviews 33, 87-99.

Lane, C.S., Brauer, A., Blockley, S.P.E., Dulski, P., 2013a. Volcanic ash reveals time-transgressive abrupt climate change during the Younger Dryas. Geology 41, 1251-1254.

Lane, C.S., Chorn, B.T., Johnson, T.C., 2013b. Ash from the Toba supereruption in Lake Malawi shows no volcanic winter in East Africa at 75 ka. Proceedings of the National Academy of Sciences 110, 8025-8029.

Lane, C.S., Cullen, V., White, D., Bramham-Law, C., Smith, V., 2014. Cryptotephra as a dating and correlation tool in archaeology. Journal of Archaeological Science 42, 42-50.

Lowe, D.J., 2011. Tephrochronology and its application: a review. Quaternary Geochronology 6, 107-153.

Machida, H., 2002. Quaternary volcanoes and widespread tephras of the world. GLOBAL ENVIRONMENTAL RESEARCH-ENGLISH EDITION- 6, 3-18.

Machida, H., Arai, F., 2003. Atlas of Tephra in and Around Japan, Univ. of Tokyo press.

Mackay, H., Hughes, P.D.M., Jensen, B.J.L., Langdon, P.G., Pyne-O'Donnell, S.D.F., Plunkett, G., Froese, D.G., Coulter, S., Gardner, J.E., 2016. A mid to late Holocene cryptotephra framework from eastern North America. Quaternary Science Reviews 132, 101-113.

MacLeod, N., Sherrod, D., Chitwood, L., Jensen, R., 1995. Geologic map of Newberry Volcano, Deschutes, Klamath, and Lake counties, Oregon. US Geological Survey.

McLean, D., Albert, P.G., Nakagawa, T., Staff, R.A., Suzuki, T., Smith, V.C., 2016. Identification of the Changbaishan 'Millennium'(B-Tm) eruption deposit in the Lake Suigetsu (SG06) sedimentary archive, Japan: Synchronisation of hemispheric-wide palaeoclimate archives. Quaternary Science Reviews 150, 301-307.

Melekestsev, I.V., Braitseva, O.A., V.V., P., Sulerzhitsky, L.D., 1996. Holocene catastrophic caldera-forming eruptions of Ksudach volcano, Kamchatka. Volcanol. Seismol. 17, 395–421.

Miller, G.H., Alley, R.B., Brigham-Grette, J., Fitzpatrick, J.J., Polyak, L., Serreze, M.C., White, J.W.C., 2010. Arctic amplification: can the past constrain the future? Quaternary Science Reviews 29, 1779-1790.

Nordli, Ø., 2010. The Svalbard airport temperature series. Bulletin of Geography. Physical Geography Series, 5-25.

Pearce, N.J., Westgate, J.A., Gatti, E., Pattan, J.N., Parthiban, G., Achyuthan, H., 2014. Individual glass shard trace element analyses confirm that all known Toba tephra reported from India is from the c. 75-ka Youngest Toba eruption. Journal of Quaternary Science 29, 729-734.

Pearce, N.J.G., Bendall, C.A., Westgate, J.A., 2008. Comment on “Some numerical considerations in the geochemical analysis of distal microtephra” by A.M. Pollard, S.P.E. Blockley and C.S. Lane. Applied Geochemistry 23, 1353-1364.

Pendea, I.F., Ponomareva, V., Bourgeois, J., Zubrow, E.B., Portnyagin, M., Ponkratova, I., Harmsen, H., Korosec, G., 2017. Late Glacial to Holocene paleoenvironmental change on the northwestern Pacific seaboard, Kamchatka Peninsula (Russia). Quaternary Science Reviews 157, 14-28.

Pilcher, J.O.N., Bradley, R.S., Francus, P., Anderson, L., 2005. A Holocene tephra record from the Lofoten Islands, Arctic Norway. Boreas 34, 136-156.

Pilcher, J.R., Hall, V.A., McCORMAC, F.G., 1996. An outline tephrochronology for the Holocene of the north of Ireland. Journal of Quaternary Science 11, 485-494.

Plunkett, G., Coulter, S.E., Ponomareva, V.V., Blaauw, M., Klimaschewski, A., Hammarlund, D., 2015. Distal tephrochronology in volcanic regions: Challenges and insights from Kamchatkan lake sediments. Global and Planetary Change 134, 26-40.

Pollard, A., Blockley, S., Lane, C., 2006. Some numerical considerations in the geochemical analysis of distal microtephra. Applied Geochemistry 21, 1692-1714.

Pouget, S., Bursik, M., Cortés, J.A., Hayward, C., 2014. Use of principal component analysis for identification of Rockland and Trego Hot Springs tephras in the Hat Creek Graben, northeastern California, USA. Quaternary Research 81, 125-137.

Pyne-O'Donnell, S.D., Hughes, P.D., Froese, D.G., Jensen, B.J., Kuehn, S.C., Mallon, G., Amesbury, M.J., Charman, D.J., Daley, T.J., Loader, N.J., 2012. High-precision ultra-distal Holocene tephrochronology in North America. Quaternary Science Reviews 52, 6-11.

Pyne-O'Donnell, S., 2011. The taphonomy of Last Glacial–Interglacial Transition (LGIT) distal volcanic ash in small Scottish lakes. Boreas 40, 131-145.

RCoreTeam, 2014. R: a language and environment for statistical computing. Vienna, Austria: R Foundation for Statistical Computing; 2012. Open access available at: http://cran. r-project. org.

Reimer, P.J., Bard, E., Bayliss, A., Beck, J.W., Blackwell, P.G., Ramsey, C.B., Buck, C.E., Cheng, H., Edwards, R.L., Friedrich, M., 2013. IntCal13 and Marine13 radiocarbon age calibration curves 0–50,000 years cal BP. Radiocarbon 55, 1869-1887.

Renssen, H., Seppä, H., Crosta, X., Goosse, H., Roche, D., 2012. Global characterization of the Holocene thermal maximum. Quaternary Science Reviews 48, 7-19.

Sejrup, H.P., Seppä, H., McKay, N.P., Kaufman, D.S., Geirsdóttir, Á., de Vernal, A., Renssen, H., Husum, K., Jennings, A., Andrews, J.T., 2016. North Atlantic-Fennoscandian Holocene climate trends and mechanisms. Quaternary Science Reviews 147, 365-378.

Serreze, M.C., Barry, R.G., 2011. Processes and impacts of Arctic amplification: A research synthesis. Global and Planetary Change 77, 85-96.

Šmilauer, P., Lepš, J., 2014. Multivariate Analysis of Ecological Data Using CANOCO 5. Cambridge university press.

Smith, V.C., Staff, R.A., Blockley, S.P., Ramsey, C.B., Nakagawa, T., Mark, D.F., Takemura, K., Danhara, T., 2013. Identification and correlation of visible tephras in the Lake Suigetsu SG06 sedimentary archive, Japan: chronostratigraphic markers for synchronising of east Asian/west Pacific palaeoclimatic records across the last 150 ka. Quaternary Science Reviews 67, 121-137.

Song, S.-R., Chen, C.-H., Lee, M.-Y., Yang, T., Iizuka, Y., Wei, K.-Y., 2000. Newly discovered eastern dispersal of the youngest Toba Tuff. Marine Geology 167, 303-312.

Sun, C., Plunkett, G., Liu, J., Zhao, H., Sigl, M., McConnell, J.R., Pilcher, J.R., Vinther, B., Steffensen, J.P., Hall, V., 2014. Ash from Changbaishan Millennium eruption recorded in Greenland ice: Implications for determining the eruption's timing and impact. Geophysical Research Letters 41, 694-701.

Ter Braak, C., 1988. CANOCO-a FORTRAN Programme for Canonical Community Ordination by [partial][detrended][canonical] Correspondence Analysis, Principal Components Analysis and Redundancy Analysis (version 2.1). Agricultural Mathematics Group.

Tomlinson, E.L., Arienzo, I., Civetta, L., Wulf, S., Smith, V.C., Hardiman, M., Lane, C.S., Carandente, A., Orsi, G., Rosi, M., 2012. Geochemistry of the Phlegraean Fields (Italy) proximal sources for major Mediterranean tephras: implications for the dispersal of Plinian and co-ignimbritic components of explosive eruptions. Geochimica et Cosmochimica Acta 93, 102-128.

Turney, C.M., 1998a. Extraction of rhyolitic component of Vedde microtephra from minerogenic lake sediments. Journal of Paleolimnology 19, 199-206.

Turney, C.S.M., 1998b. Extraction of rhyolitic component of Vedde microtephra from minerogenic lake sediments. Journal of Paleolimnology 19, 199-206.

USGS, 2005. Volcanoes, 01-09-2005 ed.

van der Bilt, W.G., D'Andrea, W.J., Bakke, J., Balascio, N.L., Werner, J.P., Gjerde, M., Bradley, R.S., 2016a. Alkenone-based reconstructions reveal four-phase Holocene temperature evolution for High Arctic Svalbard. Quaternary Science Reviews.

van der Bilt, W.G.M., Bakke, J., Balascio, N.L., 2016b. Mapping sediment–landform assemblages to constrain lacustrine sedimentation in a glacier-fed lake catchment in northwest Spitsbergen. Journal of Maps 12, 985-993.

van der Bilt, W.G.M., Bakke, J., Vasskog, K., D'Andrea, W.J., Bradley, R.S., Ólafsdóttir, S., 2015a. Reconstruction of glacier variability from lake sediments reveals dynamic Holocene climate in Svalbard. Quaternary Science Reviews 126, 201-218.

van der Bilt, W.G.M., Bakke, J., Vasskog, K., D`Andrea, W.J., 2015b. A full Holocene record of glacier variability on Svalbard reveals a dynamic Holocene in the Arctic, 45th International Arctic Workshop, p. 107.

Volynets, O., Ponomareva, V., Braitseva, O., Melekestsev, I., Chen, C.H., 1999. Holocene eruptive history of Ksudach volcanic massif, South Kamchatka: evolution of a large magmatic chamber. Journal of Volcanology and Geothermal Research 91, 23-42.

Zaretskaya, N.E., Ponomareva, V.V., Sulerzhitsky, L.D., 2007. Radiocarbon dating of large Holocene volcanic events within South Kamchatka (Russian Far East). Radiocarbon 49, 1065-1078.

Zdanowicz, C.M., Zielinski, G.A., Germani, M.S., 1999. Mount Mazama eruption: Calendrical age verified and atmospheric impact assessed. Geology 27, 621-624.

Supplementary material

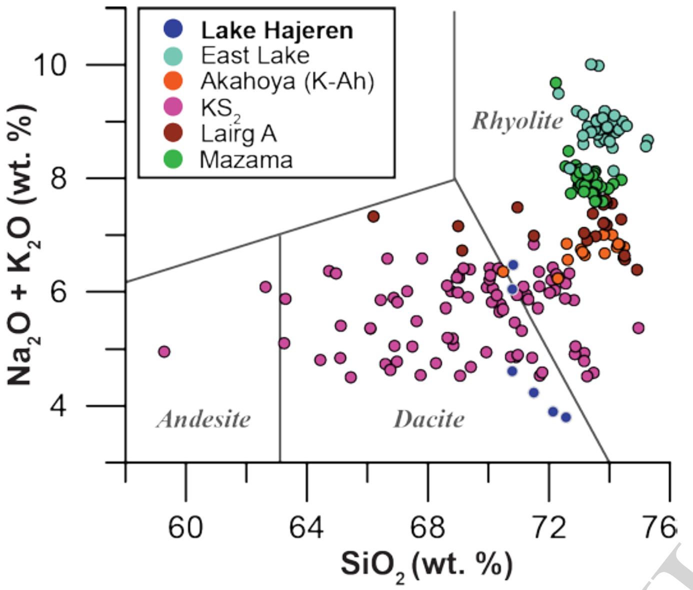

Fig. S1. Bivariate plot of normalized total alkali (Na_2O + K_2O) versus Silica (SiO_2) content for the analyzed shards from Lake Hajeren as well as the eruptions discussed in the text. Andesite, dacite and rhyolite fields are indicated and highlighted in the figure after e.g. Kyle et al. (2011).

				element oxide data - weight percent (%)											
sample	**analysis**	**instrument**	**date analysed**	**SiO_2**	**TiO_2**	**Al2O_3**	**FeO**	**MnO**	**MgO**	**CaO**	**Na_2O**	**K_2O**	**P_2O_5**	**CL**	**Total**
9526	9526/1	JEOL JXA-8600	01/04/2015	68.04	0.49	14.37	3.34	0.16	0.66	2.79	4.97	1.25	0.20	0.29	96.56
	9526/6	JEOL JXA-8600	01/08/2015	66.97	0.61	13.86	3.67	0.19	0.79	2.80	4.54	1.18	0.19	0.20	95.00
	2 / 1 .	Cameca SX100	04/03/2016	69.17	0.38	13.23	3.26	0.15	0.48	2.35	5.03	1.27	0.07	*	95.39
	3 / 1 .	Cameca SX100	04/03/2016	70.18	0.42	13.73	3.10	0.15	0.49	2.59	5.43	1.20	0.09	*	97.38
	5 / 1 .	Cameca SX100	04/03/2016	67.25	0.46	13.39	3.29	0.19	0.64	2.81	4.85	1.17	0.12	*	94.17
	6 / 1 .	Cameca SX100	04/03/2016	68.85	0.48	14.21	3.64	0.16	0.74	3.20	4.70	1.29	0.13	*	97.40
mean (μ)				*68.41*	*0.47*	*13.80*	*3.39*	*0.17*	*0.63*	*2.76*	*4.92*	*1.23*	*0.13*	*	*95.98*
two standard deviations (2σ)				*2.23*	*0.14*	*0.81*	*0.41*	*0.03*	*0.23*	*0.51*	*0.56*	*0.09*	*0.09*	*	*2.43*

Tab. S1 Sample glass geochemistry data – un-normalized

				element oxide data - weight percent (%)- mean and 2σ											
standard	**n**	**instrument**	**date analysed**	**SiO_2**	**TiO_2**	**Al2O_3**	**FeO**	**MnO**	**MgO**	**CaO**	**Na_2O**	**K_2O**	**P_2O_5**	**CL**	**Total**
ATHO-G	11	JEOL JXA-8600	01/04/2015	74.96 (0.42)	0.25 (0.01)	12.13 (0.02)	3.09 (0.13)	0.11 (0.04)	0.07 (0.02)	1.7 (0.04)	4.17 (0.11)	2.73 (0.06)	0.03 (0.02)	0.05 (0.02)	99.27
StHs6/80-G	9	JEOL JXA-8600	01/04/2015	63.57 (0.19)	0.72 (0.04)	17.66 (0.17)	4.35 (0.1)	0.08 (0.03)	1.95 (0.05)	5.22 (0.04)	4.5 (0.09)	1.3 (0.03)	0.15 (0.03)	0.02 (0.01)	99.51
ATHO-G	2	JEOL JXA-8600	01/08/2016	75.21 (0.12)	0.26 (0.01)	12.41 (0.11)	3.18 (0.01)	0.12 (0.06)	0.12 (0.02)	1.66 (0.08)	3.86 (0.41)	2.66 (0.01)	0.07 (0.002)	0.05 (0.01)	99.60
StHs6/80-G	3	JEOL JXA-8600	01/08/2016	63.20 (0.14)	0.7 (0.07)	17.69 (0.22)	4.39 (0.08)	0.05 (0.02)	1.87 (0.04)	5.14 (0.03)	4.58 (0.16)	1.29 (0.03)	0.04 (0.02)	0 (0)	98.96
GOR132-G	3	JEOL JXA-8600	01/08/2016	45.12 (0.16)	0.3 (0.04)	11.16 (0.04)	10.19 (0.13)	0.14 (0.01)	22.32 (0.12)	8.29 (0.08)	0.83 (0.16)	0.02 (0.01)	0.02 (0.04)	0.01 (0.01)	98.39
LIPARI	13	Cameca SX100	04/03/2016	74.10 (1.19)	0.08 (0.01)	12.92 (0.86)	1.58 (0.27)	0.07 (0.02)	0.05 (0.02)	0.79 (0.13)	4.00 (0.44)	5.12 (0.14)	0.01 (0.01)	*	98.71
BCR2g	5	Cameca SX100	04/03/2016	51.41 (0.56)	2.27 (0.02)	13.63 (0.60)	12.50 (0.39)	0.2 (0.03)	3.61 (0.11)	7.17 (0.19)	3.31 (0.38)	1.80 (0.11)	0.35 (0.03)	*	99.26
pooled and weighted two standard deviation (2σ)				*0.72*	*0.03*	*0.56*	*0.22*	*0.03*	*0.05*	*0.12*	*0.29*	*0.10*	*0.02*	*	

Tab. S1 Secondary glass standard data – un-normalized